IOSR Journal of Applied Physics (IOSR-JAP)
e-ISSN: 2278-4861.Volume 16, Issue 4 Ser. 1 (Jul. – Aug. 2024), PP 20-27
www.iosrjournals.org

Spectral and Thermal Analysis of Praseodymium doped Bismuth Borate Glasses for Thermionic Applications

S.L.Meena
Ceramic Laboratory, Department of physics, Jai Narain Vyas University, Jodhpur 342001(Raj.) India
E-mail address:shankardiya7@rediffmail.com

Abstract
Glass of the system:(40-x)Bi_2O_3:10ZnO:10Li_2O:10MgO:10V_2O_5:20B_2O_3: x Pr_2O_3. (where x=1, 1.5,2 mol %) have been prepared by melt-quenching method. (where x=1,1.5 and 2 mol%) have been prepared by melt-quenching technique. The amorphous nature of the prepared glass samples was confirmed by X-ray diffraction. Optical absorption, Excitation, fluorescence spectra have been recorded at room temperature for all glass samples. Judd-Ofelt intensity parameters Ω_λ (λ=2, 4 and 6) are evaluated from the intensities of various absorption bands of optical absorption spectra. Using these intensity parameters various radiative properties like spontaneous emission probability, branching ratio, radiative life time and stimulated emission cross–section of various emission lines have been evaluated.

Keywords: *ZLMVBB Glasses, Spectral Properties, Judd-Ofelt Theory, Thermal Properties.*

Date of Submission: 13-07-2024 Date of Acceptance: 27-07-2024

I. Introduction

Rare earth ions doped in different ceramic glasses to achieve favorable potential applications in a variety of optical devices such as optical, liner, lasers, fiber amplifiers, frequency-conversion materials, laser action and laser action [1-5]. Rare earth doped bismuth borate glasses are of increasing interests in various optical applications, because of their high refractive index, high density and good physical and chemical stability and high transparency. The performance and relatively low cost of borate glasses make them attractive for most of the ordinary laser applications [6-10]. Borate glasses have excellent properties such as low phonon energy, thermal stability, chemical durability and optical stability. The high gain density in borate glasses is due to high solubility of rare earth ions in borate network. Borate glasses exhibit good mechanical property. The up-conversion of borate glasses is also compressed because of their relatively large phonon energy[11-15].Pr^{3+} doped glasses have attracted much interest due to their important optical properties used in lasers, optical amplifiers, photonic devices and as infrared sensors [16-19].

The addition of network modifier (NWF) Li_2O is to improve both mechanical electrical and electrical properties of borate glasses. With the presence of property modifying (MgO) with B_2O_3 glass network could significantly improve different properties like mechanical strength, chemical durability and thermal stability [20-22].

In this work, the spectroscopic properties of Pr^{3+} -doped :(40-x)Bi_2O_3:10ZnO:10Li_2O:10MgO:10V_2O_5:20B_2O_3: x Pr_2O_3 (where x=1, 1.5,2 mol %) glasses were investigated. I have studied on the Optical absorption, Excitation, fluorescence spectra and DTA thermogram of Pr^{3+} doped zinc lithium magnesium vanadium bismuth borate glasses. The intensities of the transitions for the rare earth ions have been estimated successfully using the Judd-Ofelt theory, The laser parameters such as radiative probabilities(A),branching ratio (β), radiative life time(τ_R) and stimulated emission cross section(σ_p) are evaluated using J.O. intensity parameters(Ω_λ, λ=2,4 and 6).

II. Experimental Techniques

Preparation of glasses

The following Pr^{3+} doped zinc lithium magnesium vanadium bismuth borate glass samples :(40-x)Bi_2O_3:10ZnO:10Li_2O:10MgO:10V_2O_5:20B_2O_3: x Pr_2O_3 (where x=1, 1.5.2) have been prepared by melt-quenching method. Analytical reagent grade chemical used in the present study consist of Bi_2O_3,ZnO, Li_2O,MgO,V_2O_5, $B_2O_3$and Pr_2O_3. All weighed chemicals were powdered by using an Agate pestle mortar and mixed thoroughly before each batch (10g) was melted in alumina crucibles in silicon carbide based an electrical furnace.

Silicon Carbide Muffle furnace was heated to working temperature of 970^0C, for preparation of zinc lithium magnesium vanadium bismuth borate glasses, for two hours to ensure the melt to be free from gases. The

melt was stirred several times to ensure homogeneity. For quenching, the melt was quickly poured on the steel plate & was immediately inserted in the muffle furnace for annealing. The steel plate was preheated to100^0C.While pouring; the temperature of crucible was also maintained to prevent crystallization. And annealed at temperature of 350^0C for 2h to remove thermal strains and stresses. Every time fine powder of cerium oxide was used for polishing the samples. The glass samples so prepared were of good optical quality and were transparent. The chemical compositions of the glasses with the name of samples are summarized in Table 1

Table 1 Chemical composition of the glasses

Sample	Glass composition (mol %)
ZLMVBB (UD)	$40Bi_2O_3$:10ZnO:$10Li_2O$:10MgO:$10V_2O_5$:$20B_2O_3$
ZLMVBB PR (01)	$39Bi_2O_3$:10ZnO:$10Li_2O$:10MgO:$10V_2O_5$:$20B_2O_3$:$1Pr_2O_3$
ZLMVBB PR (1.5)	$38.5Bi_2O_3$:10ZnO:$10Li_2O$:10MgO:$10V_2O_5$:$20B_2O_3$:1.5Pr2O3
ZLMVBB PR (02)	$38Bi_2O_3$:10ZnO:$10Li_2O$:10MgO:$10V_2O_5$:$20B_2O_3$:$2Pr_2O_3$

ZLMVBB (UD)-Represents undoped Zinc Lithium Magnesium Vanadium Bismuth Borate glass specimen.
ZLMVBB (PR) -Represents Pr^{3+}Zinc Lithium Magnesium Vanadium Bismuth Borate glass specimens.

III. THEORY

3.1 Oscillator Strength

The intensity of spectral lines are expressed in terms of oscillator strengths using the relation [23].

$$f_{expt.} = 4.318 \times 10^{-9} \int \varepsilon(\nu)\, d\nu \quad (1)$$

where, ε (*ν)* is molar absorption coefficient at a given energy *ν* (cm^{-1}), to be evaluated from Beer–Lambert law.

Under Gaussian Approximation, using Beer–Lambert law, the observed oscillator strengths of the absorption bands have been experimentally calculated, using the modified relation [24].

$$P_m = 4.6 \times 10^{-9} \times \frac{1}{cl} \log \frac{I_0}{I} \times \Delta\upsilon_{1/2} \quad (2)$$

where c is the molar concentration of the absorbing ion per unit volume, I is the optical path length, $\log I_0/I$ is absorbtivity or optical density and $\Delta\upsilon_{1/2}$ is half band width.

3.2. Judd-Ofelt Intensity Parameters

According to Judd [25] and Ofelt [26] theory, independently derived expression for the oscillator strength of the induced forced electric dipole transitions between an initial J manifold $|4f^N (S, L) J\rangle$ level and the terminal J' manifold $|4f^N (S',L') J'\rangle$ is given by:

$$\frac{8\Pi^2 mc\bar{\upsilon}}{3h(2J+1)} \frac{1}{n}\left[\frac{(n^2+2)^2}{9}\right] \times S(J, J') \quad (3)$$

where, the line strength S (J, J') is given by the equation

$$S(J, J') = e^2 \sum \Omega_\lambda \langle 4f^N (S, L) J \| U^{(\lambda)} \| 4f^N (S', L') J' \rangle^2 \quad (4)$$
$$\lambda = 2, 4, 6$$

In the above equation m is the mass of an electron, c is the velocity of light, *ν* is the wave number of the transition, h is Planck's constant, n is the refractive index, J and J' are the total angular momentum of the initial and final level respectively, Ω_λ (λ = 2, 4 and 6) are known as Judd-Ofelt intensity parameters.

3.3.Radiative Properties

The Ω_λ parameters obtained using the absorption spectral results have been used to predict radiative properties such as spontaneous emission probability (A) and radiative life time (τ_R), and laser parameters like fluorescence branching ratio (β_R) and stimulated emission cross section (σ_p).

The spontaneous emission probability from initial manifold $|4f^N (S', L') J'\rangle$ to a final manifold $|4f^N (S, L) J\rangle$ is given by:

$$A[(S', L') J'; (S, L) J] = \frac{64\pi^2\nu^3}{3h(2J'+1)} \left[\frac{n(n^2+2)^2}{9}\right] \times S(J', J) \quad (5)$$

Where, $S(J', J) = e^2 [\Omega_2 \| U^{(2)} \|^2 + \Omega_4 \| U^{(4)} \|^2 + \Omega_6 \| U^{(6)} \|^2]$

The fluorescence branching ratio for the transitions originating from a specific initial manifold $|4f^N (S', L') J'\rangle$ to a final many fold $|4f^N (S, L) J\rangle$ is given by

$$\beta[(S', L') J'; (S, L) J] = \sum \frac{A[(S' L') J' (S L)]}{A[(S' L') J' (S L)]} \quad (6)$$

S L J

where, the sum is over all terminal manifolds.

The radiative life time is given by

$$\tau_{rad} = \sum_{S\ L\ J} A[(S', L')\ J'; (S,L)\ ] = A_{Total}^{-1} \quad (7)$$

where, the sum is over all possible terminal manifolds. The stimulated emission cross -section for a transition from an initial manifold $|4f^N (S', L')\ J'>$ to a final manifold $|4f^N (S, L)\ J>|$ is expressed as

$$\sigma_p(\lambda_p) = \left[\frac{\lambda_p^4}{8\pi c n^2 \Delta\lambda_{eff}}\right] \times A\left[(S', L')\ J'; (\underline{S}, \underline{L})\underline{J}\right] \quad (8)$$

where, λ_p the peak fluorescence wavelength of the emission band and $\Delta\lambda_{eff}$ is the effective fluorescence line width.

3.4 Nephelauxetic Ratio (β) and Bonding Parameter ($b^{1/2}$)

The nature of the R-O bond is known by the Nephelauxetic Ratio (β') and Bonding Parameters ($b^{1/2}$), which are computed by using following formulae [27,28]. The Nephelauxetic Ratio is given by

$$\beta' = \frac{\nu_g}{\nu_a} \quad (9)$$

where, ν_a and ν_g refer to the energies of the corresponding transition in the glass and free ion, respectively. The values of bonding parameter $b^{1/2}$ are given by

$$b^{1/2} = \left[\frac{1-\beta'}{2}\right]^{1/2} \quad (10)$$

IV. Result and Discussion

4.1. XRD Measurement

Figure 1 presents the XRD pattern of the samples containing show no sharp Bragg's peak, but only a broad diffuse hump around low angle region. This is the clear indication of amorphous nature with in the resolution limit of XRD instrument

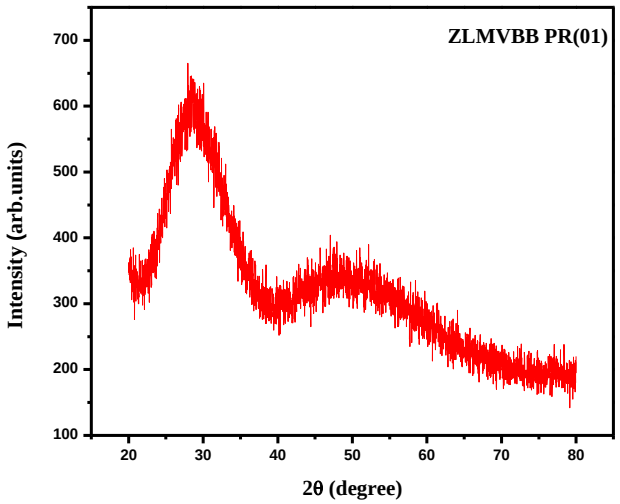

Fig.1: X-ray diffraction pattern of ZLMVBB PR (01) glass.

4.2 Thermal Properties

Fig. 2 depicts the DTA thermogram of powdered ZLMVBB sample show an endothermic peak corresponding to glass transition event followed by an exothermic peak related to crystallization event. The glass transition temperature (T_g), onset crystallization temperature (T_x), crystallization temperature (T_c) were estimated to be 520^0C, 580^0C and 598^0C respectively. From the measured value of T_g, T_x and T_c, the glass stability factor ($\Delta T = T_x - T_g$) has been determined to be 60^0C indicating the good stability of the glass.

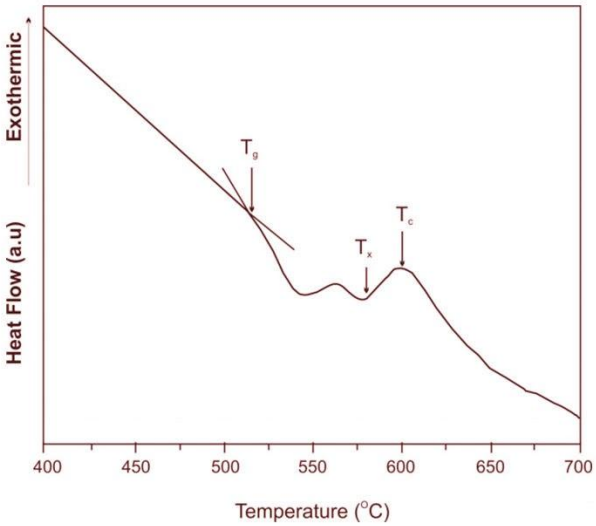

Fig.2: DTA thermogram of powdered ZLMVBB PR (01) sample.

Obtained results indicate that by increasing the amount of mol% Pr_2O_3, the T_g of the samples also increases, the small increase of T_g in these glasses shows that the structure is strongly and progressively modified. The thermal stabilities ΔT of the ZLMVBB reference glass and Pr^{+3}doped ZLMVBB glass has been evaluated from their T_g, T_c and T_c values, the results are listed out in Table 2.Hruby's parameter also calculated by using eq. (11), the greater values of the Hruby's parameter indicate higher glass forming tendency, the values of H in glasses increased with the addition of the Pr_2O_3.Eqs. (12) and (13) present the GS parameter of Weinberg [29]and Lu and Liu [30], respectively.

$$H=\frac{T_X-T_g}{T_c-T_X} \quad (11)$$

$$K_W=\frac{T_X-T_g}{T_c} \quad (12)$$

$$K_{LL}=\frac{T_X}{T_g+T_c} \quad (13)$$

Table 2: Thermal parameters determined from the DTA traces of ZLMVBB (PR) glasses.

Sample Name	% Pr_2O_3	$T_g{}^0C$	$T_X{}^0C$	$T_C{}^0C$	ΔT	H	K_W	K_{LL}
ZLMVBB (PR 1.0)	1	520	580	598	60	3.333	0.1003	0.5188
ZLMVBB (PR 1.5)	1.5	521	582	600	61	3.389	0.1017	0.5192
ZLMVBB (PR 02)	2	524	586	604	62	3.444	0.1026	0.5195

4.3. Absorption spectra

The absorption spectra of ZLMVBB (PR) glasses, consists of absorption bands corresponding to the absorptions from the ground state $^3H_4$ of Pr^{3+} ions. Eight absorption bands have been observed from the ground state $^3H_4$ to excited states $^3F_2$, $^3F_3$, $^3F_4$, $^1G_4$, $^1D_2$, $^3P_0$, $^3P_1$ and $^3P_2$ for Pr^{3+} doped ZLMVBB (PR) glasses.

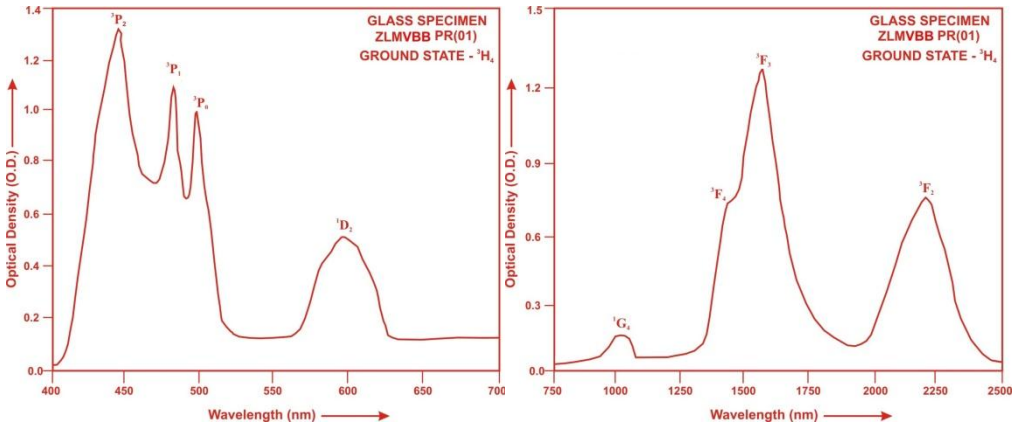

Fig.3: Absorption spectra of ZLMVBB PR (01) glass.

The experimental and calculated oscillator strengths for Pr^{3+} ions in zinc lithium magnesium vanadium bismuth borate glasses are given in **Table 3**

Table 3. Measured and calculated oscillator strength ($P^m \times 10^{+6}$) of Pr^{3+} ions in ZLMVBB glasses.

Energy level $^3H_4$	Glass ZLMVBB (PR01)		Glass ZLMVBB (PR1.5)		Glass ZLMVBB (PR02)	
	$P_{exp.}$	$P_{cal.}$	$P_{exp.}$	$P_{cal.}$	$P_{exp.}$	$P_{cal.}$
$^3F_2$	4.53	3.77	3.65	3.02	2.55	2.08
$^3F_3$	6.90	5.96	5.85	4.99	4.84	4.11
$^3F_4$	4.38	3.78	3.44	3.13	2.53	2.57
$^1G_4$	0.49	0.31	0.36	0.26	0.25	0.21
$^1D_2$	2.43	1.07	1.99	0.89	1.39	0.73
$^3P_0$	4.58	1.31	3.69	1.21	2.58	1.06
$^3P_1$	4.73	2.38	3.89	2.13	2.83	1.82
$^3P_2$	12.75	3.54	11.65	2.96	10.33	2.45
R.m.s.deviation	3.6172		3.3021		2.8835	

Computed values of Slater-Condon, Lande′, Racah, nephelauexetic ratio and bonding parameter for Pr^{3+} doped ZLMVBB glass specimens are given in **Table 4**.

Table4. Computed values of Slater-Condon, Lande′, Racah, nephelauexetic ratio and bonding parameter for Pr^{3+} doped ZLMVBB glass specimens.

Parameter	Free ion	ZLMVBB PR01	ZLMVBB PR1.5	ZLMVBB PR02
$F_2(cm^{-1})$	322.09	300.00	300.01	300.00
$F_4(cm^{-1})$	44.46	44.26	44.26	44.26
$F_6(cm^{-1})$	4.867	4.4116	4.4123	4.4116
$\xi_{4f}(cm^{-1})$	741.00	858.40	858.52	858.48
$E^1(cm^{-1})$	4728.92	4450.84	4451.02	4450.84
$E^2(cm^{-1})$	24.75	22.01	22.01	22.01
$E^3(cm^{-1})$	478.10	454.72	454.71	454.72
F_4/F_2	0.13804	0.14753	0.14753	0.14755
F_6/F_2	0.01511	0.01471	0.01471	0.01471
E^1/E^3	9.8911	9.7881	9.7887	9.7882
E^2/E^3	0.0518	0.0484	0.0484	0.0484
β'		0.88865	0.88868	0.88865
$b^{1/2}$		0.235960	0.23918	0.23596

The values of Judd-Ofelt intensity parameters are given in **Table 5**.

Table 5. Judd-Ofelt intensity parameters for Pr^{3+} doped ZLMVBB glass specimens.

Glass Specimen	$\Omega_2(pm^2)$	$\Omega_4(pm^2)$	$\Omega_6(pm^2)$	Ω_4/Ω_6
ZLMVBB PR(01)	2.827	1.848	5.379	0.3436
ZLMVBB PR(1.5)	2.130	1.706	4.441	0.3848
ZLMVBB PR(02)	1.221	1.494	3.659	0.4083

4.4 Excitation Spectrum

Excitation spectra of ZLMVBB PR (01) glass recorded at the emission wavelength 395 nm is depicted as figure 4. The excitation spectra consists of three peaks corresponding to the transitions from the ground state $^3H_4$ to the various excited states $^3P_2$, $^3P_1$ and $^3P_0$ at the wavelengths of 448, 465 and 486 nm respectively. Among these, a prominent excitation band at 448 nm has been selected for the measurement of emission spectrum of Pr^{3+} glass.

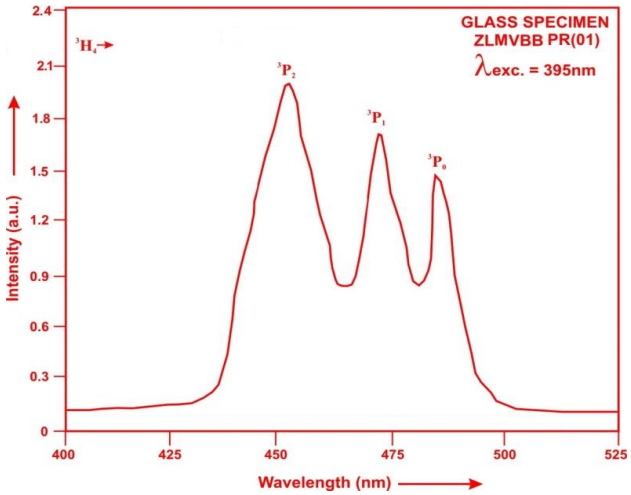

Fig.4: Excitation Spectrum of ZLMVBB PR (01) glass.

4.5. Fluorescence Spectrum

The fluorescence spectrum of ZLMVBB PR (01) doped in zinc lithium magnesium vanadium bismuth borate glass is shown in Figure 5. There eleven broad bands ($^3P_0 \rightarrow {}^3H_4$), ($^3P_0 \rightarrow {}^3H_5$), ($^1D_2 \rightarrow {}^3H_4$) ($^3P_0 \rightarrow {}^3H_6$), ($^3P_0 \rightarrow {}^3F_2$), ($^3P_1 \rightarrow {}^3F_3$), ($^1D_2 \rightarrow {}^3H_5$), ($^3P_0 \rightarrow {}^3F_4$), ($^1G_4 \rightarrow {}^3H_5$), ($^1G_4 \rightarrow {}^3H_6$) and ($^1G_4 \rightarrow {}^3F_4, {}^3F_2$) respectively for glass specimens.

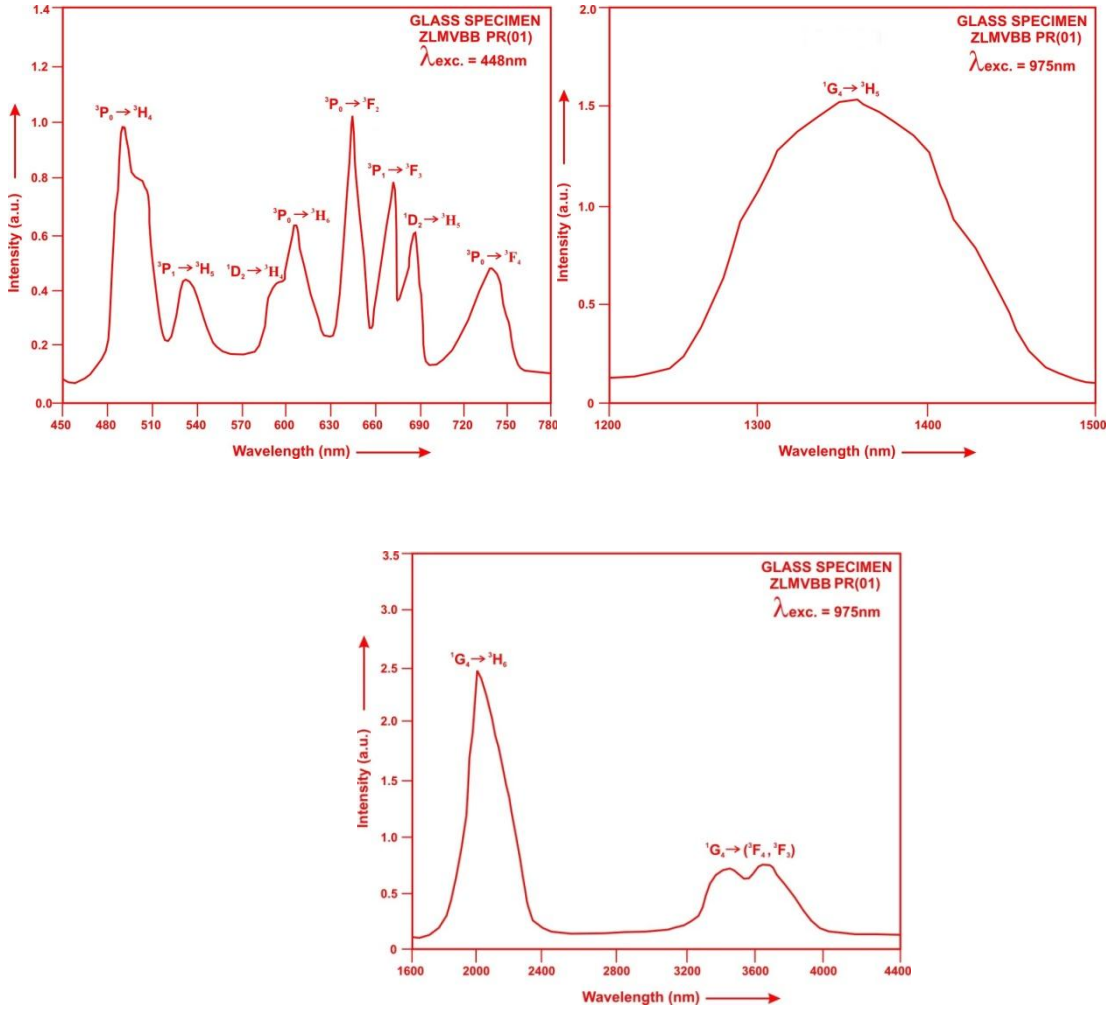

Fig.5: Fluorescence spectrum of ZLMVBB PR (01) glass.

Table 6. Emission peak wave lengths (λ_p), radiative transition probability (A_{rad}), branching ratio (β_R), stimulated emission crosssection (σ_p), and radiative life time (τ) for various transitions in Pr^{3+} doped ZLMVBB glasses.

Transition		ZLMVBB (PR)				ZLMVBB (PR)				ZLMVBB (PR)			
	λ_{max} (nm)	$A_{rad}(s^{-1})$	β	σ_p (10^{-20} cm^2)	$\tau_R(\mu s)$	$A_{rad}(s^{-1})$	β	$\sigma_p(10^{-20}$ $cm^2)$	τ_R (μs)	$A_{rad}(s^{-1})$	β	σ_p (10^{-20} cm^2)	τ_R (10^{-20} cm^2)
$^3P_0 \rightarrow {}^3H_4$	485	1088.55	0.1094	0.416		976.60	0.1196	0.445		824.67	0.1409	0.446	
$^3P_1 \rightarrow {}^3H_5$	532	2094.85	0.2106	0.448		1816.65	0.2225	0.412		1488.12	0.2542	0.356	
$^1D_2 \rightarrow {}^3H_4$	599	523.94	0.0527	0.222		439.07	0.0538	0.192		347.08	0.0593	0.166	
$^3P_0 \rightarrow {}^3H_6$	602	460.55	0.0463	0.268		383.36	0.0470	0.241		301.74	0.0515	0.216	
$^3P_0 \rightarrow {}^3F_2$	643	2081.63	0.2093	2.146	100.54	1592.10	0.1950	1.879	122.48	924.86	0.1580	1.301	170.82
$^3P_1 \rightarrow {}^3F_3$	676	3078.99	0.3096	1.788		2431.35	0.2978	1.529		1553.13	0.2653	1.056	
$^1D_2 \rightarrow {}^3H_5$	685	5.542	0.00056	0.0066		4.840	0.00059	0.0064		3.991	0.00068	0.0061	
$^3P_0 \rightarrow {}^3F_4$	730	201.08	0.0202	0.162		180.40	0.0221	0.154		152.34	0.0260	0.138	
$^1G_4 \rightarrow {}^3H_5$	1350	250.21	0.0252	0.874		208.67	0.2556	0.746		163.52	0.0279	0.598	
$^1G_4 \rightarrow {}^3H_6$	2025	142.96	0.0144	5.512		116.79	0.0143	4.680		85.07	0.0145	3.626	
$^1G_4 \rightarrow {}^3F_4, {}^3F_2$	3555	18.272	0.0018	3.745		14.54	0.0018	3.080		9.490	0.0016	2.078	

V. Conclusion

In the present study, the glass samples of composition :(40-x)Bi_2O_3:10ZnO:10Li_2O:10MgO:10V_2O_5:20B_2O_3: x Pr_2O_3 (where x =1, 1.5, 2 mol %) have been prepared by melt-quenching method. The stimulated emission cross-section (σ_p) has highest value for the transition ($^1G_4 \rightarrow {}^3H_6$) in all the glass specimen doped with Pr^{3+}ion. This shows that ($^1G_4 \rightarrow {}^3H_6$) transition is most probable transition and it useful for laser action. Large thermal stabilities (ΔT) shows that the prepared glass samples is useful for Thermionic Applications.

References

[1]. Meena,S.L.(2024). Spectral and Thermal Properties of Tm^{3+} Doped in ZincLithiumTungstenAntimonyBorophosphateGlasses, J.Appl.Phys.16 (1), 10-15.

[2]. Mandal, P.,Aditya,S.and Ghosh,S.(2020).Optimization of rare earth(Er^{3+}) doping level in lead zinc phosphate glass through Judd-Ofelt analysis,Materials Chem. And Phy., 246, 122802,1-7.

[3]. Meena,S.L.(2023). Spectral and Raman Analysis of Er^{3+} doped Ytterbium Zinc Lithium Sodalime Magnesium Borophosphate Glasses, In. J. Inn. Res. Sci.,Eng. and Tech.,12,10915-24.

[4]. Kaur,R.,Rakesh,R.B.,Mhatre,S.G.,Bhatia,V.,Kumar,D.,Singh,H.,Singh,S.P.andKumar,A. (2021). Physical, optical, structural and thermo luminescence behaviour of borosilicate glasses doped with trivalent neodymium ions, 117, 111109.

[5]. Hongisto, M., Vebar, A., Botti,N.G., Danto, S.,Jubera,V.and Petita,L.(2020).Transparent Yb^{3+} doped phosphate glass ceramics, Ceremics International 46(16),26317-26325.

[6]. Kumar,G.R. and Rao,C.S.(2020). Influence of Bi_2O_3, Sb_2O_3 and Y_2O_3 on optical properties of Er_2O_3-doped CaO–P_2O_5–B_2O_3 glasses, , Bull. Mater. Sci. 43:71, 1-7.

[7]. Meena.S.L.(2024).Structural, physical and optical properties of Pr^{3+} doped in bismuth borate glasses,Appl.Phys,130:404,1-12.

[8]. Rani,P.R., Venkateswarlu, M., Mahamuda,S., Swapna, K., Deopa, N., Rao, A., (2019).Spectroscopic studies of Dy^{3+} ions doped barium lead alumino fluoro borate glasses. J. Alloys Compd.787,503-518.

[9]. Hassaan, M. Y., Saudi, H.A., Gomaa, H.M. and Morsy, A.S. (2020). Optical Properties of Bismuth Borate Glasses Doped with Zinc and Calcium Oxides, J. of Mat. and App.,9(1),46-54.

[10]. Murthy Goud, K. K, Ramesh, C.H. and Appa Rao , B. (2017).Up conversion and Spectroscopic Properties of Rare Earth Codoped Lead Borate Glass Matrix. Material Science Research India, 14, 140-145.

[11]. Meena,S.L.(2020).Spectroscopic Properties of Er^{3+} Doped Zinc Lithium Arsenic Strontium Vanadium Bismuth Borate Glasses,Iosr Appl.Phys.12(6),5-10

[12]. Mahamuda,Sk., Swapna,K., Srinivasa Rao,A., Jayasimhadri,M., Sasikala, T.(2013). Spectroscopic properties and luminescence behavior of Nd^{3+} doped zinc alumino bismuth borate glasses, J.of Phys.and Chem.74,1308-1315.

[13]. Mohan, S. and Thind, K. S. (2017). Optical and spectroscopic properties of neodymium doped cadmium-sodium borate glasses Opt, Laser Technol. 95, 36–41

[14]. Monisha,M.,Nancy, A.,Souza, D.,legde, V.,Prabhu, N.S. and Sayyed,M.I.(2020).Dy^{3+} doped SiO_2- B_2O_3-Al_2O_3-NaF-ZnF_2 glasses , An exploration of optical and gamma radiation shielding features, Current Applied Physics 20(11), 1207-1210.

[15]. Balakrishna, A., Rajesh, D. and Ratnakaram, Y.C. (2013). Structural and optical properties of Nd^{3+} in lithium fluoro-borate glass with relevant modifier oxides. Opt. Mater.,35, 2670–2676.

[16]. Sun, Y.,Yu, F., Liao, M., Wang, X., Li, Y., Hu, L.,(2020). Knight, J. Emission properties of Pr^{3+}-doped aluminosilicate glasses at visible wavelengths. J. Lumin. 220, 117013.

[17]. Sharma, R.; Rao, A.S.; Deopa, N.; Venkateswarlu, M.; Jayasimhadri, M.; Haranath, D.; Vijaya Prakash, G. Spectroscopic study of Pr^{3+} ions doped zinc lead tungsten tellurite glasses for visible photonic device applications. Opt. Mater. 2018, 78, 457–464.

[18]. Charfi, B., Damak, K., Maâlej, R., Alqahtani, M.S., Hussein, K.I., Alshehri, A.M., Hussain, A.M., Burtan-Gwizdala, B., Reben, M., Yousef, E.S.(2022). Enhancement of Optical Telecommunication Bands: Pr^{3+}-Doped Halide Phosphate Glasses Display Broadband NIR Photoluminescence Emission. Materials, 15, 6518.

[19]. Morassuti, C.Y., Andrade, L.H.C., Silva, J.R., Baesso, M.L., Guimaraes, F.B., Rohling, J.H., Nunes, L.A.O., Boulon, G., Guyot, Y., Lima, S.M.(2019). Spectroscopic investigation and interest of Pr^{3+}-doped calcium aluminosilicate glass. J. Lumin., 210, 376–382.
[20]. Pavani, P. G., Sadhana, K. and Mouli, V. C. (2011).Optical, physical and structural studies of boro-zinc tellurite glasses, Physica B: Condensed Matter, 406, 7, 1247.
[21]. Devi, R. and Jayasankar, C. K.(1995).Optical properties of Nd^{3+} ions in lithium borate glasses, Materials chemistry and physics, 42,106-119.
[22]. Anjaiah, J. and Laxmikanth, C. (2015). Optical Properties of Neodymium Ion Doped Lithium Borate Glasses, 5,173 -183.
[23]. Gorller-Walrand, C. and Binnemans, K. (1988). Spectral Intensities of f-f Transition. In: Gshneidner Jr., K.A. and Eyring, L., Eds., Handbook on the Physics and Chemistry of Rare Earths, Vol. 25, Chap. 167, North-Holland, Amsterdam, 101.
[24]. Sharma, Y.K., Surana, S.S.L. and Singh, R.K. (2009). Spectroscopic Investigations and Luminescence Spectra of Sm^{3+} Doped Soda Lime Silicate Glasses. Journal of Rare Earths, 27, 773.
[25]. Judd, B.R. (1962). Optical Absorption Intensities of Rare Earth Ions. Physical Review, 127, 750.
[26]. Ofelt, G.S. (1962). Intensities of Crystal Spectra of Rare Earth Ions. The Journal of Chemical Physics, 37, 511.
[27]. Sinha, S.P. (1983). Systematics and properties of lanthanides, Reidel, Dordrecht.
[28]. Krupke, W.F. (1974).IEEE J. Quantum Electron QE, 10,450.
[29]. Weinberg, M.C.(1994). Experimental test of surface nucleated crystal growth modelinlithiumdiborate glass, Phys. Chem. Glasses 35, 119.
[30]. Lu, Z.P. and Liu, C.T.(2003).Glass Formation Criterion for Various Glass-Forming Systems Phys. Rev. Lett. 91,11550 .